HEATING D IONS TO OPTIMAL D-T FUSION ENERGIES IN JET-ILW

E. LERCHE^{1,2}, M. MASLOV¹, PH. JACQUET¹, I. MONAKHOV¹, D. KING¹, D. KEELING¹, C. D. CHALLIS¹, D. VAN EESTER², P. MANTICA³, C. MAGGI¹, J. GARCIA^{1,4}, F. AURIEMMA⁵, R. COELHO⁶, I. COFFEY^{1,7}, A. CHOMICZEWSKA⁸, E. DELABIE⁹, R. DUMONT⁴, P. DUMORTIER^{1,2}, J. ERIKSSON¹⁰, J. FERREIRA⁶, M. FITZGERALD¹, Z. GHANI¹, N. HAWKES¹, J. HOBIRK¹², PH. HUYNH⁴, T. JOHNSON¹³, A. KAPPATOU¹², Y. KAZAKOV², V. KIPTILY¹, K. KIROV¹, M. LENNHOLM¹, E. DE LA LUNA¹⁴, J. MAILLOUX¹, M. MARIN¹¹, G. MATTHEWS¹, S. MENMUIR¹, J. MITCHELL¹, M. NOCENTE^{3,15}, J. ONGENA², E. PARR¹, A. PATEL¹, G. PUCELLA¹⁶, D. RIGAMONTI³, F. RIMINI¹, M. SCHNEIDER¹⁷, S. SILBURN¹, M. SALEWSKI¹⁸, E. R. SOLANO¹⁴, Z. STANCAR¹, M. TARDOCCHI³, M. VALISA⁵, N. VIANELLO⁵, D. YADYKIN¹³ AND JET CONTRIBUTORS* and THE EUROFUSION TOKAMAK EXPLOITATION TEAM**

- ¹ UKAEA, CCFE, Culham Campus, Culham, UK; e-mail: Ernesto.Lerche@ukaea.uk
- ² Laboratory for Plasma Physics, ERM/KMS, Brussels, Belgium, e-mail: <u>Ernesto.Lerche@mil.be</u>
- ³ Institute of Plasma Science and Technology, Milano, Italy
- ⁴CEA, IRFM, St-Paul-Lez-Durance, France
- ⁵ Consorzio RFX ISTP-CNR, Padova, Italy
- ⁶ IPFN, Instituto Superior Tecnico, Universidade de Lisboa, Lisbon, Portugal
- ⁷ Queen's University, Belfast, UK
- ⁸ Institute of Plasma Physics and Laser Microfusion, Warsaw, Poland
- ⁹Oak Ridge National Laboratory, Oak Ridge, USA
- ¹⁰ Department of Physics and Astronomy, Uppsala University, Uppsala, Sweden
- ¹¹ EPFL, Swiss Plasma Center (SPC), Lausanne, Switzerland
- ¹² Max-Planck-Institut für Plasmaphysik, Garching, Germany
- ¹³ Fusion Plasma Physics, EES, KTH, Stockholm, Sweden
- ¹⁴ Laboratorio Nacional de Fusión, CIEMAT, Madrid, Spain
- ¹⁵ Physics Department, University of Milano-Bicocca, Milano, Italy
- ¹⁶ ENEA, Fusion and Nuclear Safety Department, Frascati, Italy
- ¹⁷ ITER organisation, St. Paul-lez-Durance Cedex, France
- ¹⁸ Technical University of Denmark, Kongens Lyngby, Denmark
- * See the author list of C.F. Maggi et al 2024 Nucl. Fusion 64 112012
- ** See the author list of E. Joffrin et al 2024 Nucl. Fusion 64 112019

Abstract

In JET-ILW, beam-target reactions contribute to a large fraction of the fusion power generated in Deuterium – Tritium (D-T) plasmas, with core ion temperatures of 10-12keV and large neutral-beam injection (NBI) power. Previous modelling done in preparation for the recent D-T campaigns in JET have shown that injecting D beam ions with energies of ~120keV in T-rich plasmas produces larger 14MeV fusion yield than in 50:50 D:T plasmas, but such scenario had never been tested in past D-T experiments. In addition, the simulations showed that fundamental ion-cyclotron resonance heating (ICRH) of the D ions can significantly boost the net fusion reactivity, since both the D-bulk ions and the fast D-beam ions are accelerated to energy ranges that are optimal for the D-T reactions to take place. In the last JET D-T campaigns (DTE2 and DTE3), dedicated experiments confirmed - for the first time - the improved fusion performance of T-rich plasmas with high D-NBI power and highlighted the key impact of fundamental D ICRH on the fusion performance. This new scenario led to the world-wide D-T fusion energy record ever achieved in a fusion device and allowed to sustain more than 12MW of fusion power averaged over 5s. The main results of these unprecedented experiments will be presented and the NBI+ICRF physics responsible for the high fusion performance achieved will be highlighted through numerical modelling.

1. INTRODUCTION

Thermonuclear reactors rely on the bulk Deuterium (D) and Tritium (T) fuel ions to reach sufficiently high temperatures for efficient fusion energy production. Under these conditions, fusion-born alpha particles are expected to produce sufficient heating to sustain the 'burning' plasma thus minimizing the need for excessive auxiliary plasma heating [1]. Another approach is to heat one of the fuel ions to supra-thermal energies using neutral beam injection (NBI) or ion cyclotron resonance heating (ICRH) while keeping the other fuel ion species at lower temperatures than the ones required for optimal thermonuclear reactions. This is commonly referred to in the literature as beam-target fusion, where the 'beam' particles are either the neutral beam injected ions (NBI) or the subpopulation of the bulk fuel ions accelerated to high energies by ICRH or both, including NBI+ICRH synergistic effects. The best D:T isotope ratio for such scenario is not 50:50 D:T, as for thermonuclear fusion, the

fusion yield being maximized when operating with larger fractions of the thermal (target) ions. While this approach is not be efficient for a steady state thermonuclear reactor, since the auxiliary power P_{aux} has to be applied continuously hence limiting the fusion gain $Q_{fus}=P_{fus}/P_{aux}$, it can be interesting for achieving the burnthrough conditions faster in reactor test facilities such as ITER [2] and BEST [3] and is particularly attractive for neutron source devices designed for plasma material research, such as the Volumetric Neutral Source (VNS) [4]. This approach was explored in the JET-ILW tokamak during the second (DTE2) [5] and third (DTE3) [6,7] Deuterium-Tritium experimental campaigns. Tritium-rich hybrid plasmas with B_0 =3.85T / I_P =2.5MA and low core collisionality were heated with D-NBI an ICRH resonating with the D ions in the plasma core [8,9]. These experiments featured the highest D-T neutron production in DTE2 and in DTE3 and led to the world-record fusion energy produced in a tokamak (E_{fus} =69MJ), with approximately 12.4MW of fusion power for 5s with P_{NBI} =30MW and P_{ICRH} =5.5MW ($Q_{fus,5s}$ =0.38). This scenario was chosen after early numerical simulations indicated that this regime was the most promising for enhancing D-T fusion reactions in JET, since the injected D-NBI ions (E_{source} =110keV) as well as the acceleration of the D_{bulk} and D_{beam} ions by ICRH are expected to drive a substantial amount of the D ions to energies close to the maximum cross-section for D-T reactions, E=50-200keV [10].

Figure 1 shows the D-T fusion power (a) and the corresponding NBI+ICRF power waveforms (b) of a series of T-rich hybrid discharges performed in DTE2 (blue) and in DTE3 (red). The full colour curves represent the fusion energy records obtained in DTE2 and DTE3, #99971 ($P_{fus}>_{5s}=10$ MW, $E_{fus}=59$ MJ) and #104522 ($P_{fus}>_{5s}=12.4$ MW, $P_{fus}=69$ MJ), respectively. The light colour pulses are other similar discharges illustrating the good reproducibility of this scenario in both campaigns, with several pulses producing large fusion energy values. Note how the fusion power responds promptly to the input power waveform, a typical feature of a beam-target dominant fusion scenario. Neutron spectroscopy measurements as well as numerical simulations show that $\sim 80\%$ of the D-T power comes from NBI+ICRF driven 'beam'-target reactions in these pulses. The main improvement in DTE3 allowing for higher fusion energies was the higher and steadier input power, in particular in discharge #104522 which featured steady $P_{NBI}=30$ MW and $P_{ICRH}=5.5$ MW throughout. The reduced fusion performance seen in the light-coloured pulses around t=10s are related to trips in the NBI power, as can be observed in panel (b).

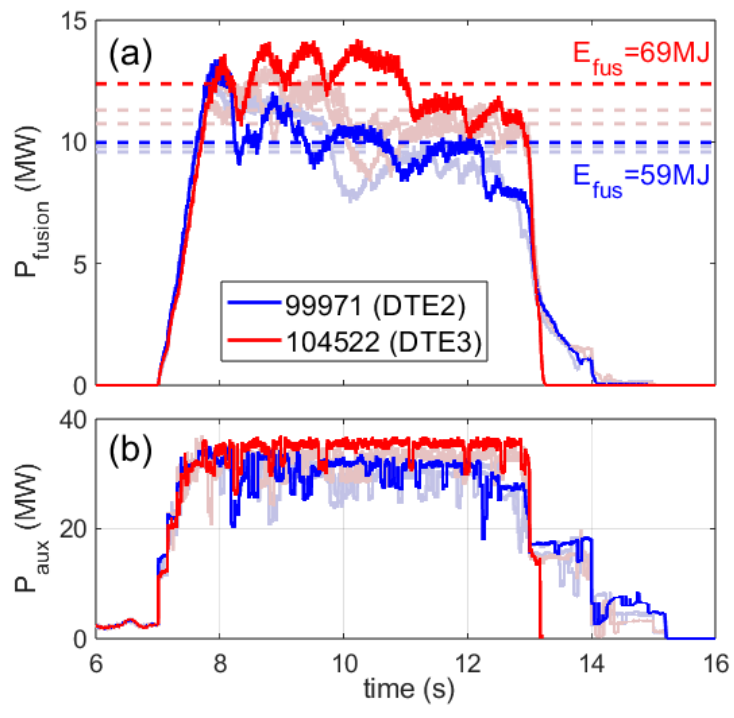


FIG. 1. D-T fusion power (a) and auxiliary input power (b) for various T-rich discharges performed in DTE2 (blue) and DTE3 (red). Pulses #99971 and #104522 represent the fusion energy records obtained in DTE2 and DTE3, respectively.

Going from a T-rich plasma to a 50:50 D:T plasma showed a clear decrease in the beam-target fusion yield, not because of the lower ICRF heating efficiency with large D fractions but due to a combination of weaker D_{bulk} acceleration and less T target ions for the fast D ions to collide with. This was the first time that fundamental D heating was applied to a 50:50 D:T plasma, which is relevant for its potential use in ITER [11].

The physics governing the generation of the fast D ion tails generated by NBI+ICRF heating in these experiments and their impact on the total D-T fusion yield in JET-ILW will be discussed based on state-of-the-art numerical simulations using the Heating & Current Drive (H&CD) modules of the European Transport Solver (ETS) [12]. The simulations results will be benchmarked against the experimental findings from T-rich and from 50:50 D:T plasmas in JET, highlighting the optimal conditions for beam-target neutron generation.

2. THE T-RICH FUSION RECORD SCENARIO

Hybrid plasmas [13] with low shear q-profile in the plasma centre ($q_0 \ge 1$, $q_{95} = 4-5$) were used as backbone for the high-performance T-rich scenario presented here [8]. High confinement is obtained by exploring a high β_{pol} regime while keeping β_N relatively low to mitigate neoclassical tearing modes, with a plasma current of I_P =2.5MA and a magnetic field of B_0 =3.85T, allowing for fundamental D ICRF heating at f=29MHz in the core. The plasma density is relatively low, n_{e0} =(7-8)x10¹⁹/m³, so that the NBI power deposition is peaked, leading to T_{i0} > T_{e0} in general. Deuterium NBI was used (P_{NBI} ≈28-30MW, E_{source} ~110keV) and the discharges were fuelled with T_2 gas only, leading to an isotope ratio of approximately 15%D:85%T due to the D-NBI thermalization.

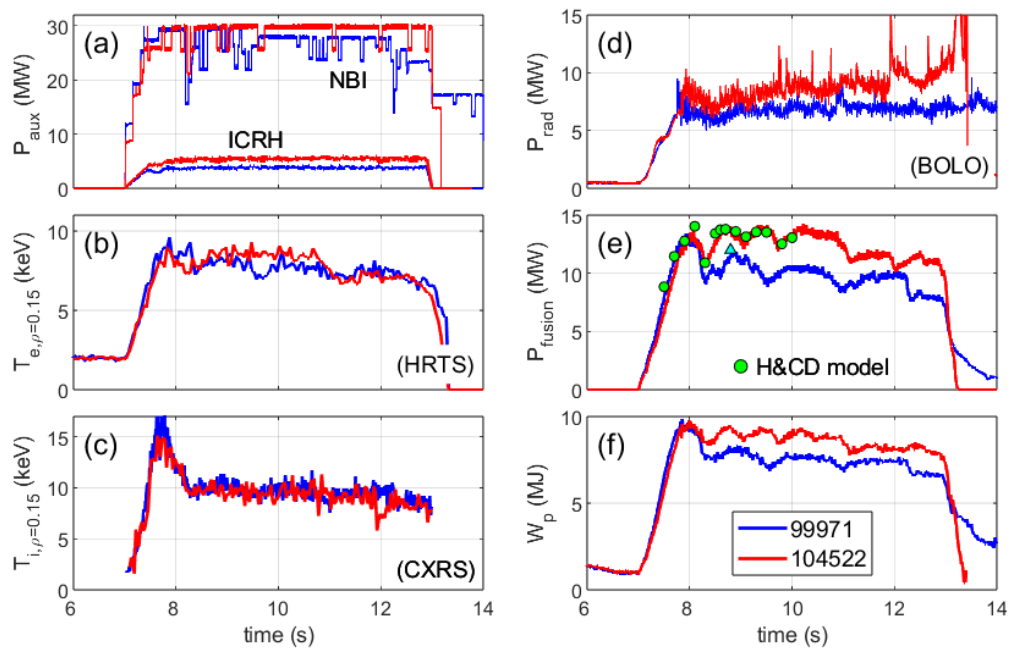


FIG. 2: Time traces of the best performing T-rich hybrid pulses in DTE2 (#99971) and in DTE3 (#104522): (a) NBI and ICRF power; (b) Central electron temperature (HRTS); (c) Central ion temperature (CXRS); (d) Bulk radiated power (bolometer); (e) D-T Fusion power; (f) Plasma stored energy. The points in panel (e) show the fusion power calculated with the ETS H&CD simulations using the experimental input parameters.

Figure 2 compares the new T-rich fusion record shot (#104522) obtained in DTE3 with the previous record obtained in DTE2 (#99971). Both discharges were almost identical from the engineering point of view except for the input power (a): The NBI power is roughly the same (~30MW) up to t=9s but the NBI set-up was different in the two discharges. One injector (~2MW) is lost in #99971 after t=9s while the power remains constant in pulse #104522. In addition, the ICRF transmission lines were thoroughly conditioned to operate at higher voltages in DTE3 allowing to increase the ICRF power from P_{ICRH}=4MW to 5.5MW in DTE3. The impact on the central electron (b) and ion (c) temperatures is small, but the fusion power is substantially increased: During the matched NBI power phase (t<9s) with additional 1.5MW of ICRH, about 1.5MW of extra fusion power (e) is produced, most of it due to the stronger ICRF acceleration of the D_{bulk} and D_{nbi} ions. Later in the discharge, when on top of the higher ICRH power discharge #104522 features an additional 2MW of NBI, the fusion power difference is even larger reaching ~3.5MW at t=10s. This shows how efficient this heating scenario is for beam-target fusion power generation, in particular when combined NBI+ICRH is used. The plasma stored energy (f) is also higher in #104522 due to wider temperature profiles and a larger fraction of fast particles with more ICRH, as will be discussed later. The bulk radiation (d) is also larger in #104522 as a consequence of the higher input power leading to stronger plasma-wall interaction, but the discharge is still stable from the impurity accumulation point of view until t=10.5s. After this, the central electron temperature starts decreasing (and the central SXR emission, not shown, increases), but the impact on central $T_i(c)$, $W_P(f)$ and $P_{fusion}(e)$ is still relatively small. At t=12s there is a large impurity event in pulse #104522 which leads to core impurity accumulation, density peaking and a disruption after approximately 1.5s. The slightly less performing discharges executed in DTE3 also shown in Fig.1 (#104520 with E_{fus} =63MJ and 104675 with E_{fus} =66MJ), in which there was no impurity event, did not suffer from impurity peaking and could be successfully terminated around t=15s.

Figure 3 compares the radial kinetic profiles measured in pulses #99971(o) and #104522(\square) at t=8.6s. The electron density (a) is comparable although somewhat less peaked in #104522. The electron temperature (b) and particularly the ion temperature profile (c), are clearly broader in the new pulse but the NBI injector needed for central CX measurements was missing so that the central T_i values estimated from CXRS (at ρ =0.15) are similar

(Fig.2c). The broader T_i profile observed in pulse #104522 is consistent with the broader NBI deposition profile calculated by ASCOT (d) due to the different NBI configuration used and also due to the increased off-axis ICRF absorption calculated for pulse #104522, as will be discussed later.

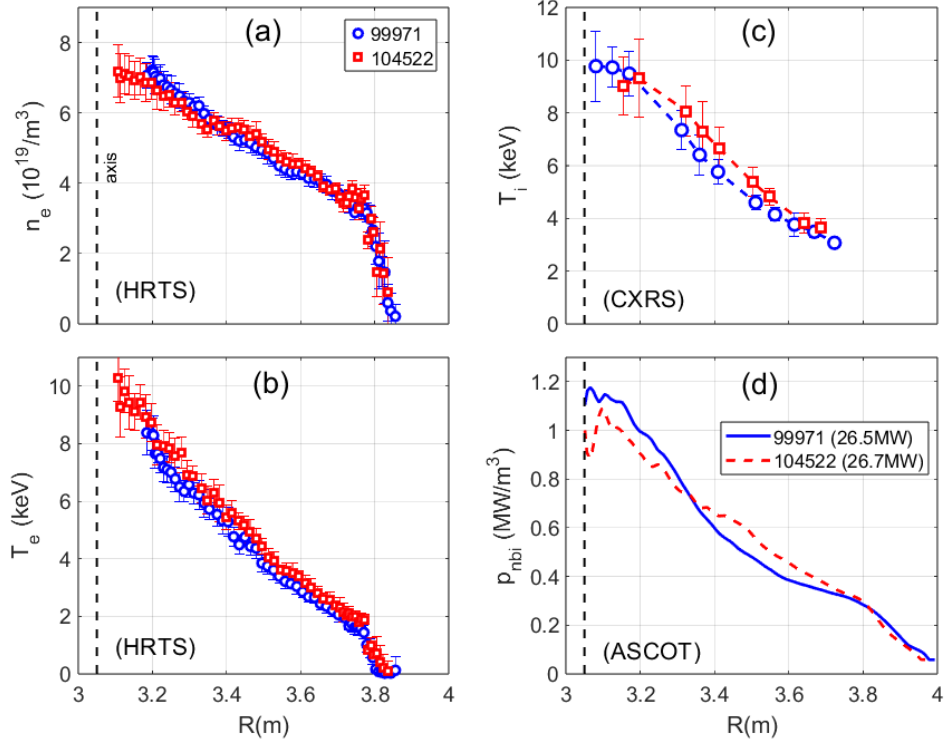


FIG. 3: Kinetic profiles measured for pulses #99971 (o) and #104522 (\square) at t=8.6s: (a) Electron density (HRTS); (b) Electron temperature (HRTS); (c) Ion temperature (CXRS); (d) NBI deposition profiles (ASCOT)

The experimental parameters of discharge #104522 were used to perform NBI+ICRH heating simulations of the T-rich plasmas using the Heating & Current Drive (H&CD) modules from the *European Transport Solver* (ETS) [12]. The kinetic profiles were fitted from a combination of the available diagnostics data and the equilibrium was computed with a pressure constrained EFIT simulation. A radially uniform 15% Deuterium concentration was assumed, with 0.5% of Beryllium and 0.1% of Nickel. The H&CD workflow was executed as follows: First, the NBI deposition was computed using the ASCOT code [14], considering the 3 beam energy fractions as independent ion species. The NBI losses (reionizaton, shine-through, etc.) are discarded and only the remaining 'slowing-down' power (P_{NBI} =26.6MW) is retained in the simulations. The ICRH power absorption profiles for all species (including the three NBI energy components) are computed using the 2D full wave CYRANO code [15], assuming P_{ICRH} =5.5MW is absorbed in the plasma. Finally, the obtained RF-fields and power absorption profiles are used as input for the Fokker-Planck code FOPLA [16], which computes the accelerated distribution functions of all the ions (including self-collisions) and the collisional power repartition of the ICRF and NBI power to the bulk plasma. The fusion power is then calculated using the converged distribution functions of all the ion species present in the plasma.

The results are summarized in Fig. 4, where the NBI deposition and the ICRH power absorption profiles (a) are plotted together with the collisional power redistribution profiles (b) computed for pulse #104522 at t=8.6s. The ICRF power absorption previously calculated for pulse #99971 (with P_{ICRH}=4MW) is shown as dotted curves in Fig.4 (a) while the total power absorbed by each species is compared in the legend. One sees that most of the additional ICRF power in pulse #104522 is actually absorbed by the D_{beam} ions (+1.2MW) starting at ρ_{norm} =0.3 while only ~0.3MW is added to the bulk D ion absorption. This is due to the larger off-axis beam population present in pulse #104522 which is characterized by a broader NBI deposition due to the different NBI settings (see Fig.3d). It's interesting to note that because of the localized nature of the ICRH absorption, it represents a substantial heat source in the plasma center, with peak power density values comparable to the NBI ones despite the almost 5 times lower power injected in the plasma. The central ICRH absorption is still dominated by the bulk D ions but the D_{beam} ions absorb ~60% of the total ICRF power due to their broad (Doppler-shifted) power absorption. In Fig.4 (b), the dotted curves illustrate the collisional power profiles obtained with NBI only for pulse #104522 with otherwise identical parameters as the NBI+ICRH calculations (solid curves). Bulk ion heating is already dominant with NBI only heating (Pelec=10.2MW, Pion=16.4MW) since the beams are injected with E~110keV and the critical energy is about 150keV in these conditions. From the additional 5.5MW of ICRH applied, ca. 2.3MW are collisionally transferred to the electrons and 3.2MW to the bulk D+T ions. The peaked power absorption by electrons in the plasma core may be less interesting for fusion enhancement but is beneficial for core impurity screening [17], rendering the high power ICRH discharges more stationary than others with less ICRF power. The fraction of ICRF power that contributes as bulk ion heat source is also peaked in the centre and has a strong impact on the core ion temperature and on the total fusion yield, as discussed later.

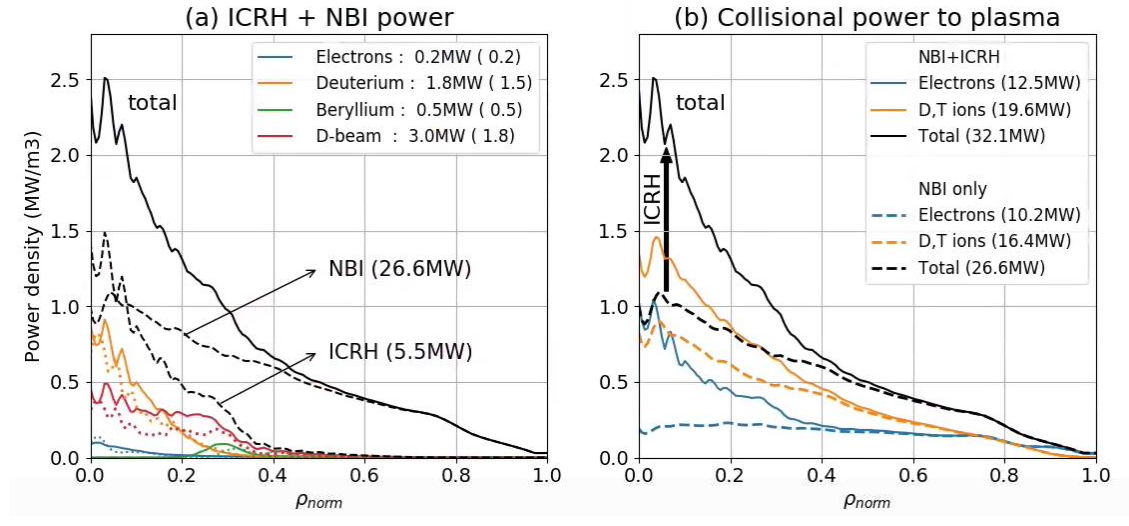


FIG. 4. (a) ICRH wave power absorption profiles for the different plasma species for the parameters of pulse #104522 (DTE3) at t=8.6s. The dotted curves in (a) represent the profiles calculated for #99971 (DTE2); (b) Collisional power transferred to the bulk plasma for pulse #104522. The dashed curves in (b) represent the results obtained without ICRH (NBI only).

As shown before, the additional 1.5MW of ICRH power coupled to pulse #104522 as compared to #99971 had a strong impact on the fusion performance (Fig.2). In Figure 5, the D-T fusion power profiles calculated for pulses #104522 (a) and #99971 (b) at t=8.6s are compared. They were computed using the converged distribution functions of all the ion species calculated by the Fokker-Planck code FOPLA after several iterations. The dotted curves show the results obtained without ICRH (NBI only) while the solid curves represent the actual ICRH+NBI simulations with 5.5MW and 4.0MW as in the experiments, respectively. The D-T neutron calculations for pulse #99971 (Fig.5-b) are shown for comparison purposes only and were already discussed extensively in [9,18]. From Fig.5a one sees that from the 5.5MW of ICRH power applied, a remarkable 3.5MW are 'converted' into fusion power (Q_{RF}=0.64), with roughly equilibrated contribution to the thermal + ICRH (D_{bulk}+D_{fast}) and to the beamtarget (including ICRF synergy) reaction channels. In the plasma centre, the thermal + ICRH enhancement is larger due to the efficient acceleration of bulk D ions to supra-thermal energies, as reported in [9]. When compared to #99971 (b), one sees that the extra +1.5MW of ICRF power applied in #104522 is primarily added to the beamtarget channel (~1MW), which is consistent with the larger D_{beam} absorption shown in Fig.4a due to the broader NBI deposition profile computed for #104522 by the ASCOT code (Fig.3d).

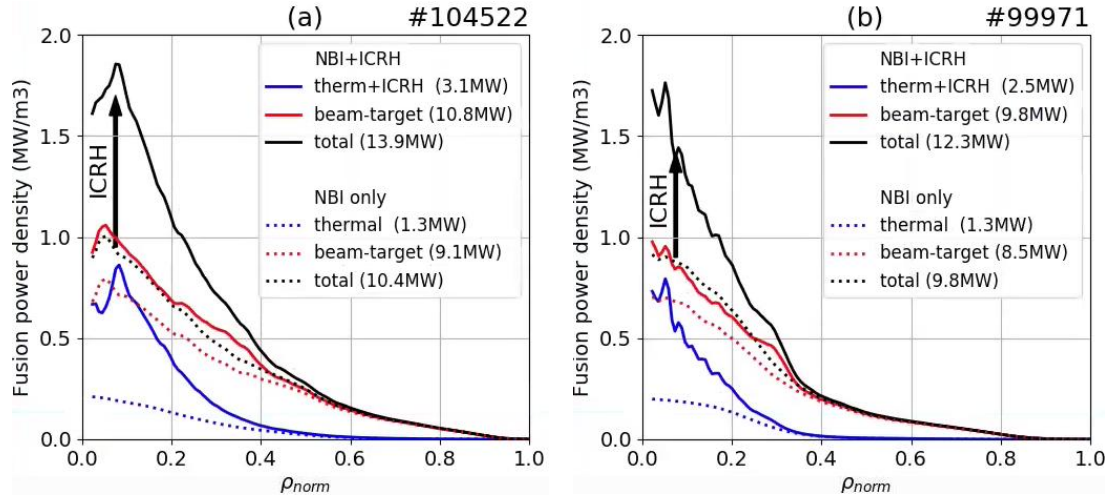


FIG. 5: Fusion power density profiles obtained with the H&CD ETS workflow for pulses #104522 (a) and #99971 (b). The dotted curves represent the results with \sim 26.5MW of NBI-only heating while the solid curves show the results with NBI+ICRH, with P_{ICRH} =5.5MW for #104522 and P_{ICRH} =4.0MW for shot #99971.

3. IMPACT OF D:T ISOTOPE RATIO ON FUSION POWER

To illustrate the advantage of a T-rich plasma scenario for maximizing the beam-target D-T reactions and to assess the influence of the fundamental D ICRF heating scheme on D-T fusion enhancement, two similar discharges with different D:T mixtures were executed: #104523 with 15:85 D:T and #104521 with 50:50 D:T. In both cases the ICRH power was modulated at 1Hz to study the transient response of the plasma to ICRF heating. The time traces of the most relevant quantities are given in Fig 6 (left). The NBI and ICRH power waveforms (a) were similar in both cases (P_{NBI}=28/30MW, P_{ICRH}=4MW) but the fusion power (b) is about 2 times lower in the 50:50 D:T discharge. The central ion temperature (c) as well as the plasma stored energy (d) are also lower by 20-30% in the latter. Former fusion power calculations done prior to the experiment [9] predicted a reduction of the fusion power of ~30% when the isotope ratio was changed from 15:85 to 50:50 D:T, but they did not account for changes in the kinetic profiles nor in the plasma confinement properties. The new calculations done with the H&CD ETS tools using the actual kinetic profiles measured in these discharges with and without ICRH agree very well with the experimental results, as illustrated by the green points shown in Fig.6b. The right panels in Fig.6 show a blow-up of the time window used for the ICRH modulation studies, in which the linear background (dashed line on the left graphs) has been subtracted from the relevant signals. The horizontal lines correspond to the amplitude of the modulation of the various quantities computed with an FFT.

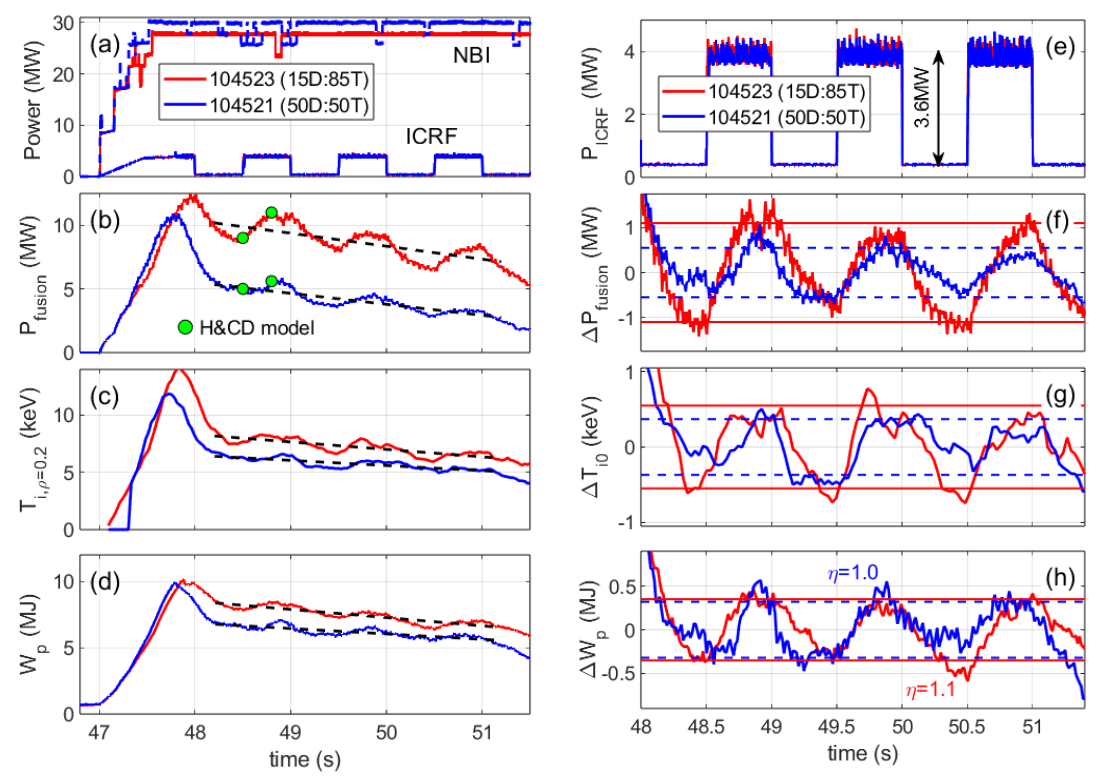


FIG. 6: Time traces of various signals comparing the fusion performance of a 15:85 D:T T-rich discharge (#104523) with a 50:50 D:T discharge (#104521): (a) Input power; (b) Fusion power; (c) Central ion temperature (CXRS, ρ =0.2); (d) Plasma stored energy; The panels on the right (e-h) show a blow-up of the same quantities and illustrate the response of the various signals to the 1Hz ICRF power modulation. The linear time evolution of the signals has been subtracted for the FFT analysis: the amplitudes are represented as horizontal lines in panels (f,g,h) for the 2 pulses.

It's interesting to note that the response of the plasma stored energy (h) is similar in both cases, $\Delta W_P = 0.7-0.8 MJ$, which suggests that the wave absorption properties did not change much when the D concentration was increased. The RF heating efficiency computed by break-in slope analysis [19] of the plasma energy response to the ICRF modulation shows indeed very similar results for the second modulation cycle, $\eta_{RF}=1.0$ (#104521) and $\eta_{RF}=1.1$ (#104523), and a somewhat reduced value in the third RF modulation cycle for the 50:50 D:T case ($\eta_{RF}=0.8$), where the D concentration starts exceeding 50%. The first ICRF cycle cannot be properly analysed in #104521 because of the NBI trips occurring at the same time. The central ion temperature response (g) is somewhat weaker in the 50:50 D:T case ($\Delta T_{i0} \approx 0.8 keV$ compared to $\Delta T_{i0} \approx 1.1 keV$) which points to the fact that the wave absorption per species is different. The ICRH simulations confirm that the D_{bulk} absorption is reduced in the 50:50 D:T case while the D_{beam} absorption is increased (the overall single-pass absorption being similar), which combined with the lower plasma temperature (lower critical energy) in the 50:50 D:T case leads to stronger

collisional electron heating. In the T-rich discharge, the D_{bulk} and D_{nbi} absorptions are more equilibrated leading to a dominant collisional ion heating scenario, similar to what was discussed in the previous section. Note that the T-rich pulse #104523 is very similar to pulse #99965 performed in DTE2 for which a detailed ICRH+NBI analysis has already been reported in [9,20]. Finally, the variation of the fusion power with the ICRH modulation (f) is very different in the two discharges: In the T-rich pulse, ΔP_{ICRH} =3.6MW leads to about $\Delta P_{fus} \approx 2.0$ MW where in the 50:50 D:T case it only produces about $\Delta P_{fus} \approx 0.8$ MW (even a bit less in the last modulation cycle). The strong reduction in the fusion power enhancement with ICRH in the 50:50 D:T discharge is due to a combination of less D_{bulk} acceleration and the reduced number of T ions available for the fast deuterons to collide with. The H&CD model captures all these aspects and hence provides a reliable prediction of the different scenarios. This is illustrated in Fig.7, which compares the fusion power density profiles calculated for the 2 discharges in question with and without ICRH. The integrated fusion power values for each case with NBI+ICRH (P_{ICRH} =4MW) and with NBI only heating (residual P_{ICRF} =0.3MW, as in the experiments) are given in the respective legends.

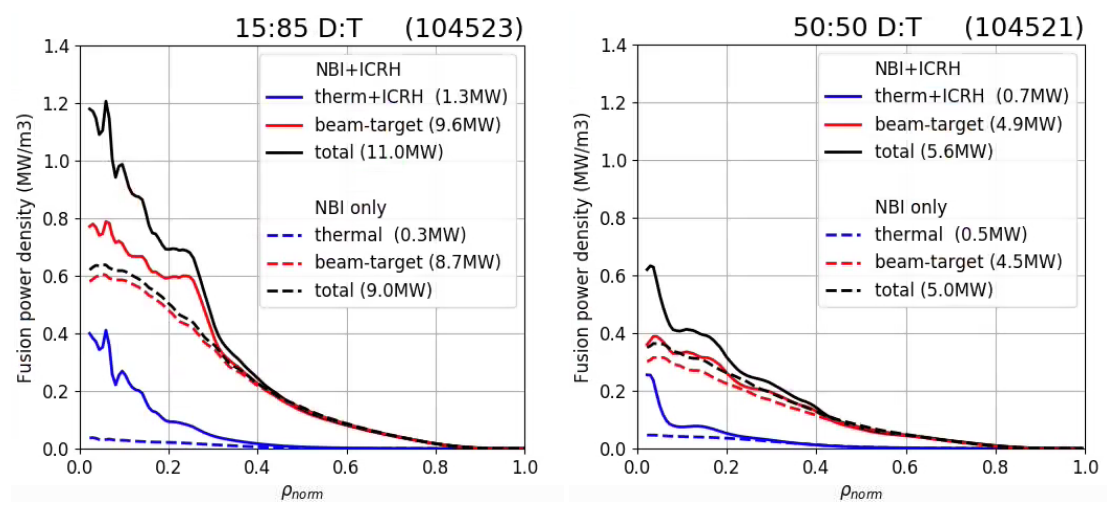


FIG. 7: D-T fusion power profiles calculated for the 15:85 D:T (#104523) and for the 50:50 D:T (#104521) discharges with 4MW of ICRH power (NBI+ICRH, solid) and with 0.3MW of residual ICRH (NBI only, dashed).

Fig.7 (left) shows a similar fusion power pattern as the one discussed in section 2 for #99971 (Fig.3), except that the NBI power is lower (P_{NBI} =28MW instead of 30MW). The ICRH power is the same (P_{ICRF} =4MW) but, because of less beam particles in the plasma, the fusion power enhancement caused by ICRH is slightly lower (ΔP_{fus} =2MW instead of 2.5MW) and it comes roughly equilibrated in terms of thermonuclear (D_{bulk} acceleration) and beam-target (D_{nbi} acceleration) reactions. For the 50:50 D:T case (Fig.7-right), the situation is dramatically different: In the absence of ICRH and despite the slightly higher NBI power than in #104523, the beam-target reactions only amount to 4.5MW, mainly because the population of Tritium (target) ions is strongly reduced. For the same reason, the thermonuclear reactions are somewhat higher than in the T-rich case (despite the lower T_i) but they are only a very small fraction of the total fusion power anyway. When 4MW of ICRH is applied, the 'thermal+ICRH' reaction channel is only increased in a small volume near the centre and the beam-target reactions are only enhanced by 0.4MW, amounting to a total fusion enhancement of 0.6MW, as seen in the experiments. This poor performance is not only due to the reduced population of T ions but also due to a lower acceleration of the large fraction of D_{bulk} ions, as mentioned earlier.

4. SUMMARY AND CONCLUSIONS

Inspired by modelling of NBI+ICRF heating and D-T fusion generation done prior to the experimental D-T campaigns in JET-ILW [9], the record D-T fusion energy production ever achieved in a tokamak was attained in the DTE2 campaign (#99971, E_{fus} =59MJ) [5] and subsequently extended in DTE3 in pulse #104522, featuring $< P_{fus} >= 12.4 \text{MW}$ for 5s and $E_{fus} = 69 \text{MJ}$ [6,7]. This record fusion performance was obtained using T-rich hybrid plasmas with $\sim 30 \text{MW}$ of D-NBI injection and with 5.5MW of ICRF heating using the fundamental Deuterium heating scheme in the plasma centre. The plasma scenario was very reproducible and several discharges reached fusion energies between 60-70MJ in DTE3. In these pulses, more than 80% of the D-T reactions came from fast D – thermal T reactions, as confirmed by neutron spectroscopy measurements [21] and by numerical H&CD modelling [9]. The fast D population was composed by D beam ions injected with $E_{source} \approx 110 \text{keV}$ (with $\sim 30 \%$ at half energy and $\sim 20 \%$ with $1/3 E_{source}$), by thermalized D ions accelerated by ICRH and by D-beam ions that are 'kicked' to higher energies by the ICRF fields during slowing-down, effectively leading to a large fraction of fast

D ions with optimal energies for D-T fusion (E=50-200keV) [10]. As expected for a dominant beam-target scenario, the fusion yield is very sensitive to the input power waveform so the best results were achieved with steadier NBI and higher ICRH power, as obtained in DTE3. Increasing the ICRH power from 4MW to 5.5MW (and using a slightly different NBI injector configuration) promptly increased the fusion power by ~1.5MW, showing how efficient this heating scheme is for producing D ions with optimal energy range for D-T fusion. The simulations indicate that 0.9MW of the fusion enhancement comes from the stronger ICRH acceleration of the D_{bulk} and D_{nbi} ions and 0.6MW comes from the broader NBI deposition obtained in DTE3. In addition, higher ICRH power increased the stationarity of the discharges, which often suffered from slow density peaking and impurity accumulation despite the fast ELM's characteristic of this scenario [8]. This was even more evident in the discharges performed with ICRH modulation which suffered from gradually decreasing performance throughout the discharge. The H&CD simulations performed within the ETS framework showed a surprisingly good agreement with the experiments in terms of fusion power predictions. The fast distribution functions of all ion species (including the 3 NBI energy components) were used to estimate the fusion power.

The same scenario was repeated with equilibrated 50:50 D:T isotope ratio and the results were strikingly underperforming. While the ion temperature and plasma stored energy were about 20-30% lower in the 50:50 D:T sibling discharge, the fusion power was reduced by a factor of two. Again, the H&CD simulations confirmed this effect both with NBI only and with NBI+ICRF heating simulations, the main reason being (i) the reduction of the number of thermal Tritium ions for the fast D ions to collide with and (ii) the weaker acceleration of the bulk D ions by ICRH with n_D/n_e =50%. The ICRF heating efficiency was surprisingly similar in the two cases, mainly because of the stronger off-axis D_{beam} absorption in the latter which compensated for the worse RF electric field polarization in the plasma center for interacting with the bulk D ions.

To summarize, plasma scenarios with dominant 'beam'-target fusion as the one described here are not directly relevant to thermonuclear reactors as such, but can be attractive for moderate Q / high fluence D-T fusion power generation. They can be used for example in devices that require high 14MeV neutron fluence for fusion reactor material studies, such as the Volumetric Neutron Source (VNS) project [4]. They can also be used in ITER and in BEST with dominant ICRF heating of D_{bulk} ions (and low NBI density) to generate moderate activation D-T scenarios (to e.g. test and calibrate the neutron diagnostics) or to assist the the entry into H-mode with an unbalanced isotope ratio by producing larger ion heat sources in the plasma. Numerical studies are being performed for these devices and will be left for a future publication.

Finally, second harmonic ICRF heating of fuel ions (either D or T) can also be envisaged to enhance the D-T fusion power, but in general these heating schemes are less efficient than fundamental ICRF heating because (i) they require the resonant ions to be pre-heated for efficient RF absorption and (ii) they typically accelerate only a small fraction of the resonant ions to very high energies [22], often exceeding those optimal for D-T reactions.

ACKNOWLEDGMENTS

This work has been carried out within the framework of the EUROfusion Consortium, funded by the European Union via the Euratom Research and Training Programme (Grant Agreement No 101052200 - EUROfusion). Views and opinions expressed are those of the author(s) and do not necessarily reflect those of the European Union or the European Commission.

REFERENCES

- [1] SALEWSKI, M. et al 2025 Nucl. Fusion 65 043002
- [2] LOARTE, A. et al 2025 Plasma Phys. Ctrl. Fus. 67 065023
- [3] YAN, J. and KONG, D. et al, Proc. of 9th IAEA DEMO and Fusion Plants Workshop, Aomori, Japan (2025)
- [4] BACHMANN, C. et al 2025 Fus. Eng. and Des. 211 114796
- [5] MAGGI C. F. et al 2024 Nucl. Fusion 64 112012
- [6] KAPPATOU, A. et al 2025 Plasma Phys. Ctrl. Fus. 67 045039
- [7] VIANELLO, N. et al, IAEA-FEC 2025, OV 2-1 (Chengdu)
- [8] MASLOV, M. et al 2023 Nucl. Fusion **63** 112002
- [9] LERCHE, E. et al, AIP Conf. Proc. 2984, 030005 (2023)
- [10] BOSCH, H.-S and HALE, G.M., 1992 Nucl. Fusion 32 611
- [11] SCHNEIDER, M. et al 2021 Nucl. Fusion 61 126058

- [12] HUYNH, P. et al 2021 Nucl. Fusion 61 096019
- [13] HOBIRK, J. et al 2023 Nucl. Fusion 63 112001
- [14] HIRVIJOKI, E. et al 2014 Comp. Phys. Comm. 185 1310
- [15] LAMALLE, P., PhD Thesis, Univ. de Mons, Belgium (1994)
- [16] VAN EESTER, D. et al 2011 Plasma Phys. Ctrl. Fus. 53 092001
- [17] LERCHE, E. et al 2016 Nucl. Fusion **56** 036022
- [18] JÄRLEBLAD, H. et al 2025 Nucl. Fusion **65** 016060
- [19] LERCHE, E. et al 2008 Plasma Phys. Ctrl. Fus. 50 035003
- [20] MANTICA, P. et al 2024 Nucl. Fusion 64 086001
- [21] NOCENTE, M. et al 2022 Review of Sci. Instr. 93(9) 093520
- [22] STIX, T. H. 1975 Nucl. Fusion 15 737